

I. TITLE PAGE

**α_{2A} Adrenergic Receptor Activation Inhibits Epileptiform Activity
in the Rat Hippocampal CA3 Region**

Chris W.D. Jurgens, Hana M. Hammad¹, Jessica A. Lichter, Sarah J. Boese,
Brian W. Nelson, Brianna L. Goldenstein, Kylie L. Davis, Ke Xu, Kristin L. Hillman,
James E. Porter² and Van A. Doze²

*Department of Pharmacology, Physiology and Therapeutics
University of North Dakota School of Medicine and Health Sciences
Grand Forks, North Dakota*

II. RUNNING TITLE PAGE

- a) Running Title:
 α_{2A} Adrenergic Receptor Inhibition of Epileptiform Activity
- b) Corresponding author:
Van A. Doze, Ph.D.
Department of Pharmacology, Physiology and Therapeutics
School of Medicine and Health Sciences
University of North Dakota
501 North Columbia Road, Stop 9037
Grand Forks, ND 58202-9037
Tel.: (701)-777-6222
Fax: (701)-777-4490
E-mail address: vdoze@medicine.nodak.edu
- c) Number of text pages: 34
Number of tables: 3
Number of figures: 5
Number of references: 40
Number of words in Abstract: 250
Number of words in Introduction: 707
Number of words in Discussion: 1500
- d) Nonstandard Abbreviations:
ACSF, artificial cerebral spinal fluid;
AR, adrenergic receptor;
ARC-239, 2-[2-(4-(2-Methoxyphenyl)piperazin-1-yl)ethyl]-4,4-dimethyl-1,3-(2*H*,4*H*)-isoquinolindione dihydrochloride;
BAPTA, 1,2-bis(2-aminophenoxy)ethane-*N,N,N',N'*-tetraacetic acid;
BRL-44408, 2-[(4,5-Dihydro-1*H*-imidazol-2-yl)methyl]-2,3-dihydro-1-methyl-1*H*-isoindole maleate;
CA3, cornu ammonis 3;
CaMKII, calcium/calmodulin-dependent protein kinase-II;
EPI, epinephrine;
6FNE, 6-fluoronorepinephrine;
GAD, glutamate decarboxylase;
GFAP, glial fibrillary acidic protein;
IR/DIC, infrared-differential interference contrast;
LTP, long-term potentiation;
MK-912, (2*S*-trans)-1,3,4,5',6,6',7,12b-octahydro-1',3'-dimethyl-spiro[2*H*-benzofuro[2,3-*a*]quinolizine-2,4'(1'*H*)-pyrimidin]-2'(3'*H*)-one hydrochloride;
NE, norepinephrine;
P, postnatal;
PHE, (R)-(-)-phenylephrine;
RT-PCR, reverse transcription-polymerase chain reaction;
UK-14304, 5-Bromo-6-(2-imidazolylamino)quinoxaline tartrate.

III. ABSTRACT

Norepinephrine has potent antiepileptic properties, the pharmacology of which is unclear. Under conditions where GABAergic inhibition is blocked, norepinephrine reduces hippocampal CA3 epileptiform activity through α_2 adrenergic receptor (AR) activation on pyramidal cells. In this study, we investigated which α_2 AR subtype(s) mediate this effect. First, α_2 AR genomic expression patterns of twenty-five rat CA3 pyramidal cells were determined using real time single cell RT-PCR, demonstrating that twelve cells expressed α_{2A} AR transcript, with three of the twelve cells additionally expressing mRNA for α_{2C} AR subtype, and no cells possessing α_{2B} AR mRNA. Hippocampal CA3 epileptiform activity was then examined using field potential recordings in brain slices. The selective α AR agonist 6-fluoronorepinephrine caused a reduction of CA3 epileptiform activity, as measured by decreased frequency of spontaneous epileptiform bursts. In the presence of β AR blockade, concentration-response curves for AR agonists suggest that an α_2 AR mediates this response, as the rank order of potency was UK-14304 \geq epinephrine > 6-fluoronorepinephrine > norepinephrine \gggg phenylephrine. Finally, equilibrium dissociation constants (K_b) of selective α AR antagonists were functionally determined to confirm the specific α_2 AR subtype inhibiting CA3 epileptiform activity. Apparent K_b values calculated for atipamezole (1.7 nM), MK-912 (4.8 nM), BRL-44408 (15 nM), yohimbine (63 nM), ARC-239 (540 nM), prazosin (4900 nM) and terazosin (5000 nM) correlated best with affinities previously determined for the α_{2A} AR subtype ($r = 0.99$, slope = 1.0). These results suggest that, under conditions of impaired GABAergic inhibition, activation of α_{2A} ARs is primarily responsible for the antiepileptic actions of norepinephrine in the rat hippocampal CA3 region.

IV. BODY OF MANUSCRIPT

Introduction

The noradrenergic system is a key modulator of numerous physiological and pathological processes. Within the central nervous system (CNS), noradrenergic neurons innervate copious neural networks and regulate a number of essential neurological functions including attention and arousal, sleep, and learning and memory (Pupo and Minneman, 2001). The CNS noradrenergic system also plays a significant role in attenuating epileptic phenomena (Giorgi et al., 2004) and is implicated in neurodegenerative diseases such as Alzheimer's and Parkinson's. The hippocampus, a limbic structure intricately involved in learning and memory, receives substantial adrenergic innervation in all subfields, including the cornu ammonis 3 (CA3) region. Numerous studies have indicated that the hippocampal CA3 region is essential for many cognitive processes including spatial pattern recognition, novelty detection and short-term memory (Kesner et al., 2004). Characteristic of the CA3 region is a dense recurrent network among the excitatory pyramidal neurons, which is believed crucial for performing these cognitive functions (Traub et al., 1991). However, the immense connectivity of the CA3 axon collaterals makes this region extremely vulnerable to overexcitation (Schwartzkroin, 1986). Indeed, the CA3 region has one of the lowest seizure thresholds in the brain and is often involved in temporal lobe epilepsy, the most common human epileptic syndrome. Therefore, strict control over the inhibitory and excitatory aspects of this network is essential.

Norepinephrine (NE), the major neurotransmitter released by noradrenergic neurons, modulates several vital hippocampal CA3 processes. Long-term potentiation (LTP), a form of activity-dependent neuronal enhancement, which is believed to underlie memory formation, is strongly facilitated by NE in the hippocampal CA3 region (Hopkins and Johnson, 1988). In addition, NE enhances certain memory processes (Murchison et al., 2004) some of which are thought to involve the CA3 region. NE also has documented antiepileptic properties (Giorgi et

al., 2004). Reduced levels of endogenous NE are associated with an increased susceptibility to seizures (Weinshenker and Szot, 2002), while increased brain NE release inhibits seizure activity (Weiss et al., 1990). Furthermore, several clinically-used antiepileptic therapies have been shown to either increase brain NE levels (Baf et al., 1994) or require intact NE innervation for their clinical efficacy (Krahl et al., 1998; Szot et al., 2001). Although the LTP/memory-enhancing and antiepileptic actions of NE have been known for many years, the mechanism by which NE mediates these effects is still unclear. Based on the differential expression of adrenergic receptor mRNA observed in hippocampal interneurons and pyramidal cells (Hillman et al., 2005a), we believe that the ability of NE to both potentiate the excitatory processes underlying memory and inhibit the aberrant overexcitation association with seizures, is achieved through the distinct and diverse expression of postsynaptic receptors on these different cell types (Hillman et al., 2005b; Jurgens et al., 2005).

NE and its major congener, epinephrine (EPI), mediate their effects through the activation of adrenergic receptors (ARs). ARs have been divided into three major classes, each of which has a unique G-protein pairing resulting in diverse physiological actions (Pupo and Minneman, 2001). Several studies have suggested that β ARs mediate NE's enhancement of LTP (Hopkins and Johnston, 1988) and memory (Devauges and Sarah, 1991), while the antiepileptic actions of NE may involve α AR activation (Weinshenker and Szot, 2002). We recently found that NE inhibits rat hippocampal CA3 epileptiform burst discharges through α_2 AR activation (Jurgens et al., 2005). Pharmacological and molecular cloning studies have revealed the existence of three α_2 AR subtypes denoted α_{2A} , α_{2B} , α_{2C} (Bylund et al., 1994). Although gene expression studies have found transcripts for all three α_2 AR subtypes in rat brain (Nicholas et al., 1993; Scheinin et al., 1994), only α_{2A} and α_{2C} AR mRNA appear to be expressed in the rat hippocampus (Winzer-Serhan and Leslie, 1997; Winzer-Serhan et al., 1997a, b).

The goal of this study was to characterize the effect of α_2 AR subtype activation on rat hippocampal CA3 network synchronization under conditions of impaired synaptic inhibition. Genomic expression patterns of α_2 AR mRNA in single hippocampal CA3 pyramidal neurons, rank order of potencies for AR agonist-mediated responses, and functional determination of subtype-selective α_2 AR antagonist equilibrium dissociation constants were used to determine the specific α_2 AR subtype involved in reducing hippocampal CA3 network activity observed in this model. Delineating which α_2 AR subtype attenuates hippocampal overexcitation (i.e., epileptic phenomena) may provide clues to help elucidate the mechanism by which NE inhibits epileptogenesis.

Materials and Methods

Reagents. BAPTA tetrapotassium salt, desipramine hydrochloride, (-)-epinephrine bitartrate salt, 6-fluoronorepinephrine hydrochloride, MK-912, (-)-norepinephrine (+)-bitartrate salt hydrate, (R)-(-)-phenylephrine hydrochloride, picrotoxin, and timolol maleate salt were obtained from Sigma-Aldrich (St. Louis, MO). ARC-239, BRL-44408, prazosin hydrochloride, terazosin [1-(4-amino-6,7-dimethoxy-2-quinazoliny)-4-[(tetrahydro-2-furanyl)carbonyl]-piperazine hydrochloride], UK-14304 and yohimbine hydrochloride were acquired from Tocris Cookston Inc. (Ellisville, MO). Atipamezole [(4-(2-ethyl-2,3-dihydro-1H-inden-2-yl)-1H-imidazole) was manufactured by Orion Corporation (Espoo, Finland). Isoflurane was ordered from Abbott Diagnostics (Chicago, IL). All chemical reagents used to make the artificial cerebral spinal fluid (ACSF) and the microelectrode solutions were of biological grade from J.T. Baker, Inc. (Phillipsburg, NJ), Fisher Scientific Co. (Fairlawn, NJ) or Sigma-Aldrich (St. Louis, MO). Unless otherwise noted, all molecular biology reagents used for single cell reverse transcription polymerase chain reaction (RT-PCR) were obtained from Promega (Madison, WI).

Animals. Sprague–Dawley rat pups were housed with their mothers in cages (size 16.5 x 8.5 inches) kept in rooms maintained at a temperature of ~22 °C with a relative humidity of ~55 %. Water and dried laboratory food (Teklad Global 18% Protein Rodent Diet; Harlan Teklad, Madison, WI) were provided *ad libitum*. Lighting was set to a 12-h light/dark cycle (lights on at 7:00 AM). Rats were allowed to acclimate for at least two days after arrival from Harlan (Indianapolis, IN) before their use. All protocols described have been approved by the Institutional Animal Care and Use Committee of the University of North Dakota in accordance with the National Institute of Health Guide for the Care and Use of Laboratory Animals.

Slice Preparation. Hippocampal brain slices were prepared from young Sprague–Dawley rats (P12–P29) weighing 25–90 g. Animals were deeply anesthetized with isoflurane, sacrificed

by decapitation, and their brains immediately removed. Hippocampi were quickly dissected from each hemisphere and placed into a 4 °C ringer solution containing, in mM: choline chloride 110, KCl 2.5, MgSO₄ 7, CaCl₂ 0.5, NaH₂PO₄ 1.25, NaHCO₃ 25, glucose 25, sodium ascorbate 11.6, and sodium pyruvate 3.1. Using a conventional tissue sectioning apparatus (Stoelting, Wood Dale, IL), the hippocampi were sectioned transversely into 500 µm thick slices (Fig. 1A) and transferred to artificial cerebral spinal fluid (ACSF) consisting of, in mM: NaCl 119, KCl 5, MgSO₄ 1.3, CaCl₂ 2.5, NaH₂PO₄ 1, NaHCO₃ 26.2, and glucose 11. The slices were incubated at 34 ± 1 °C for 30 min, and then allowed to recover for at least an additional 30 min at room temperature (22 ± 1 °C) prior to experimentation. All solutions were continually aerated with 95 % O₂:5 % CO₂.

Cytoplasm Collection. A single hippocampal slice was transferred to a perfusion chamber (Siskiyou, Grants Pass, OR) and visualized under IR/DIC optics using an Olympus BX-51WI microscope (Olympus, Melville, NY) while being constantly perfused with oxygenated ACSF at room temperature (22 ± 1 °C). A candidate hippocampal CA3 pyramidal cell was visually identified and centered in the field. A micropipette tip loaded with 50 U RNasin[®] Ribonuclease Inhibitor and back-filled with, in mM: KMeSO₄ 135, NaCl 8, Hepes 10, MgATP 2, NaGTP 0.3, and BAPTA-K₄, was driven into the tissue while applying slight positive pressure to keep the tip clear of debris and placed flush with the membrane of the candidate pyramidal cell (Fig. 1B). Applying a slight negative pressure, the membrane of the cell was disrupted and the cytoplasmic contents of the candidate cell gently aspirated, being careful not to disrupt the nucleus. The sample was immediately prepared for RT-PCR.

Single Cell RT-PCR. Single cell RT-PCR was performed as previously described (Hillman et al., 2005a) with a few small modifications. The cytoplasmic contents were expelled into a 10 µl total reaction volume containing, in final concentrations: 500 µM dNTPs, 10 mM DTT, 1× first

strand buffer, 25 U RNasin[®] Ribonuclease Inhibitor, 200 U M-MLV reverse transcriptase (Invitrogen, Carlsbad, CA), and 0.5 ng of anchored RT primer mixture (5' → 3': CTCTCAAGGATCTTACCGCT₍₁₇₎(A,G,C)N, where N represents A, C, G, or T). The reaction was incubated at 37 °C for 60 min. The resulting first strand was treated with 1 U RNase H (Promega, Madison, WI), and incubated at 37 °C for 60 min to remove hybrid dimers. Four second strand primer mixtures, 2.5 pg each, were annealed at 50 °C for 10 min. Each primer contained the base sequence TGCATCTATCTAATGCTCCNNNNNXXXXX, with differing 3' heel sequences (XXXXX) of: CGAGA, CGACA, CGTAC, and ATGCG. The second strand was then extended by adding 1 mM dNTPs, 0.5 U PfuUltra[™] Polymerase (Stratagene, La Jolla, CA), 2× PfuUltra[™] Buffer, and incubated at 72 °C for 15 min.

PCR amplification 1. 250 μM dNTPs, 0.25× PfuUltra[™] Buffer, 1.25 U PfuUltra[™] Polymerase, 2.5 μl DNase free water, 1 ng of the anchored RT primer mixture, and 1 ng of each second strand primer mixture were added to the reaction tube. Using a standard thermal cycler (Eppendorf Mastercycler[®], Westbury, NY), the reaction was subjected to a hot start step of 95 °C/2 min, followed by 15 cycles of 92 °C/1 min, 60 °C/1 min, 72 °C/1.5 min, with a final extension step of 72 °C/5 min.

PCR amplification 2. The reaction was spiked with: 1× Ex Taq[™] Buffer, 1 mM dNTPs, 2.5 U Ex Taq[™] HS Polymerase (Takara Bio Inc., Otsu, Japan), 8.5 μl DNase free water, 10 ng of the anchored RT primer mixture, and 10 ng of each second strand primer mixture. The reaction was subjected to a hot start step of 95 °C/2 min, followed by 40 cycles of 92 °C/1 min, 60 °C/1 min, 72 °C/2 min, with a final extension step of 72 °C/5 min.

Controls. The above protocol was performed on three controls during each experimental run. *Control 1:* Reverse transcriptase was omitted to ensure amplified message was representative of mRNA, and not a result of genomic amplification. *Control 2:* As a positive control, 1 ng of previously isolated hippocampal RNA (Eppendorf Perfect RNA[™], Westbury,

NY) was used in place of a cytoplasmic sample. This control consistently provided a cDNA template that gave positive gene products for all primers listed in Table 1, with the exception of STS ET3. Previously isolated hippocampal DNA, 1ng, was used to provide a positive STS ET3 control during the gene specific amplification. *Control 3:* As a negative control to ensure nonspecific amplification of the primers was not occurring, template was omitted.

Gene Specific Amplification Using Real Time PCR. 3 μ l aliquots of the final cDNA template reaction were used to determine mRNA expression patterns for AR subtypes. 3–5 μ l of cDNA template, 20 μ M each of forward and reverse gene specific primer (Table 1), 1.5 \times R-PCR™ buffer, 1 \times Cepheid Additive (0.004 mg Bovine Serum Albumin, 150 mM Trehalose, 0.2% Tween-20), 250 μ M dNTPs, 3 mM Mg²⁺, 0.25 \times SYBR green dye (BioWhittaker, Rockland, ME), and 2.5 U Ex Taq™ HS polymerase were combined and brought to 25 μ l with DNase free water. Using the Cepheid SmartCycler® System (Sunnyvale, CA), the reactions were subjected to a hot start step of 95 °C/120 s; 42 cycles of 95 °C/15 s, 57 °C/30 s, 72 °C/30 s; final extension of 72 °C/60 s. A melt curve analysis was performed on each run immediately after the extension step to determine product presence and purity (data not shown). AR characterization was only completed on samples that were positive for the housekeeping gene β -actin and negative for the genomic marker STS ET3, indicating successful amplification of cytoplasmic mRNA. All gene specific primer pairs were designed using Vector NTI® Software (San Francisco, CA) and synthesized by Integrated DNA Technologies (Coralville, IA) or Sigma-Genosys (The Woodlands, TX). Gene specific primer sequences were chosen based on minimal primer-dimer formation, high sequence specificity, and annealing temperatures within 55-60 °C.

Electrophysiological Recordings. A single slice was transferred to the recording chamber, where it was submerged and superfused continuously at a rate of ~4 mL/min with

ACSF at room temperature (22 ± 1 °C). Glass microelectrodes were made using a two-stage puller (PP-830, Narashige, Japan). Extracellular field potentials were recorded using microelectrodes filled with 3 M NaCl placed in the stratum pyramidale of the CA3 region of the hippocampus (same general area where the cytoplasmic samples were taken; see Fig. 1A). Currents were detected using an Axoclamp 2B (Axon Instruments, Union City, CA), amplified at 10× or 100× using a Brownlee Precision Model 440 instrumentation amplifier (Brownlee Precision, San Jose, CA), digitized at 1 kHz with a Digidata 1322A analog-to-digital converter (Axon Instruments), and recorded using Axoscope 9.0 software (Axon Instruments).

Generation of Epileptiform Activity. It has been established that hippocampal CA3 pyramidal neurons will fire spontaneous epileptiform burst discharges due, in part, to their extensive recurrent circuitry (Traub et al., 1991). This activity can be elicited by attenuating synaptic inhibition using a GABA_A receptor antagonist such as picrotoxin. To elicit epileptiform bursts, slices were continually superfused with ACSF containing picrotoxin (100 μM) and any applicable AR antagonist. If no burst discharges were seen after 20 min of perfusion, the slices were determined to be unresponsive and discarded. Once burst discharges were evident, 30 min of baseline data was recorded before any exposure to an AR agonist. Preliminary experiments were conducted to assure that AR antagonists showed no independent effects and that each AR agonist concentration produced its maximum effect in the time allotted (data not shown).

Data Analysis. Burst discharge frequencies were visualized in real time (Fig. 2A) while being recorded for subsequent on-line analysis. Post-experimental analysis was completed using Mini Analysis 6.0 (Synaptosoft, Decatur, GA). The last interval correlating to each agonist concentration was noted, the baseline frequency was subtracted, and that value was used to plot a concentration-response expressed as percent of maximal response. Frequency versus

agonist concentration data was then entered into GraphPad Prism 4.03 (GraphPad Software, San Diego, CA) and concentration-response curves were constructed using a non-linear least squares curve fitting method. Each curve was fit with a standard (slope = unity) or variable slope, and the best-fit was determined using an *F*-test with a value of $p < 0.05$. The calculated EC_{50} value was used as a measurement of agonist potency. Significance between groups was tested using an unpaired two-tailed Student's *t* test ($p < 0.05$).

Equilibrium dissociation constant (K_b) values for the selective α AR antagonists were estimated using the method of Schild originally described by Arunlakshana and Schild (1959). For each experiment, cumulative concentration-response curves were performed in adjacent hippocampal slices of the same rat (one concentration-response curve per slice). Dose-ratios of EC_{50} values in the presence and absence of a selective AR antagonist were calculated and Schild plots constructed by graphing the log of the dose ratio – 1 versus the log of the AR antagonist concentration (Arunlakshana and Schild, 1959). Linear regression analysis of these plotted points was used to determine the slope and x-intercept of the Schild regressions. Schild regression slopes are expressed as the mean \pm S.E. and were considered different if the 95% confidence interval did not include the value of 1 (Kenakin, 1997). The K_b values of subtype-selective α AR antagonists causing competitive inhibition of agonist initiated burst discharge frequencies were calculated from Schild regression x-intercepts. Differences in pK_b values and Schild regression slopes were determined by analysis of covariance with a $p < 0.05$ level of probability accepted as significant. Calculated values (i.e., EC_{50} and K_b) are expressed as the mean \pm S.E. for *n* experiments.

Results

Hippocampal CA3 Pyramidal Cell Characterization. Previously, it was demonstrated that NE reduces epileptiform burst activity in the hippocampal CA3 region through AR activation on pyramidal cells (Jurgens et al., 2005). Therefore, we examined the RNA expression patterns for subtypes of α_2 ARs in CA3 pyramidal cells using a single cell real time RT-PCR method designed to allow simultaneous identification of transcriptional expression patterns for neuronal cell type markers and AR subtypes (Hillman et al., 2005a). Real time PCR was employed for gene-specific amplification because its enhanced sensitivity (1 pg limit) allows the detection of multiple transcripts within a single cell sample. Listed in Table 1 are gene-specific primer pairs used to identify positive transcripts from single hippocampal CA3 pyramidal cells. Also listed in Table 1 are amplicon melt temperatures, which were subsequently used to identify positive transcripts from single cell samples. The criteria for confirming positive transcripts were: (1) the sample was free of genomic and cellular contamination; (2) the transcript product gave a fluorescence signal of at least 10 U of fluorescence over background; (3) the gene-specific PCR melt temperature was within 1 °C of positive control value (Hillman et al., 2005a). Based on these criteria, 25 cytoplasmic samples taken from individual hippocampal CA3 pyramidal cells, identified visually based on their location in the pyramidal cell layer and their characteristic pyramidal shape (Fig. 1B), were determined to have specific RT-PCR amplification products. These 25 samples were successfully amplified free of genomic contamination, as indicated by their expression of the house-keeping gene β -actin and lack of the genomic marker for a polymorphic repeat STS ET3 (Hillman et al., 2005a). The pyramidal cell origin of these samples was confirmed by the presence of mRNA transcripts for calcium/calmodulin-dependent protein kinase-II (CaMKII), an enzyme specific to pyramidal cells and/or absence of mRNA for glial fibrillary acidic protein (GFAP) and glutamate decarboxylase (GAD65), markers of astrocytes and interneurons, respectively. Of the three α_2 AR subtypes tested, the α_{2A} AR subtype was

transcriptionally expressed in 12 of the 25 samples, with three of these pyramidal cells additionally expressing α_{2C} AR mRNA (Table 2). No mRNA for the α_{2B} AR subtype was detected. Previous reports describe no α_2 AR mRNA expression in hippocampal CA1 pyramidal cells (Hillman et al., 2005a). These results summarized in Table 2, demonstrate that α_{2A} AR and/or α_{2C} AR are transcriptionally expressed in CA3 pyramidal cells.

α -AR Effects on Hippocampal CA3 Epileptiform Activity. The highly selective α AR agonist, 6-fluoronorepinephrine (6FNE), possesses an approximately 10- and 1000-fold selectivity for α_1 and α_2 ARs, respectively, when compared to β ARs (Lu et al., 2000). We first examined the effects of 6FNE on burst discharges to corroborate the type of α AR action on hippocampal activity observed in our previous studies (Jurgens et al., 2005). For these recordings, an extracellular electrode was placed in the hippocampal pyramidal cell layer in the area of the CA3 region where pyramidal cells expressing mRNA were found (Fig. 1A, top diagram). As illustrated in Fig. 2A, picrotoxin-induced epileptiform burst discharges appear as sharp biphasic spikes. The depolarizing/hyperpolarizing waveform corresponds to a series of population spikes followed by an after-hyperpolarization in CA3 pyramidal neurons (Traub et al., 1991). Application of 6FNE caused a concentration-dependent decrease in the number of these events (Fig. 2A). Using a frequency histogram of the 6FNE-induced decrease in burst discharges (Fig. 2B), a concentration-response curve was constructed from a plot of maximal burst frequency versus 6FNE concentration (Fig. 2C). For this experiment, the EC_{50} value calculated from non-linear regression analysis was 110 nM. The agonist concentration-response profile for different slices from a single animal was similar (data not shown). The mean EC_{50} value for 6FNE-induced decreased burst firing was 310 ± 86 nM, $n = 20$ (Fig. 2C). The high potency of 6FNE to reduce hippocampal CA3 network activity suggests that this effect is most likely through activation of an α AR.

Effects of Endogenous Catecholamines and other α AR agonists on Hippocampal CA3 Epileptiform Activity. Since NE and EPI are the endogenous agonists for α_2 AR mediated responses in the rat hippocampus, we compared the effects of these nonselective AR agonists to the selective α AR agonist 6FNE, the selective α_1 AR agonist phenylephrine (PHE) and the selective α_2 AR agonist UK-14304 on hippocampal CA3 burst activity frequency in the presence of β AR blockade. As illustrated in Fig. 3, after pre-treatment of slices with 10 μ M timolol to block β ARs and 0.5 μ M desipramine to block catecholamine reuptake, application of UK-14304, EPI, 6FNE, NE or PHE caused a concentration-dependent decrease in the frequency of hippocampal CA3 epileptiform burst discharges. The potency of 6FNE in the presence of timolol (300 ± 140 nM, $n = 12$; Fig. 3) was not significantly different than EC_{50} values for 6FNE calculated in the absence of β AR blockage (310 ± 86 nM, $n = 20$; Fig. 2C). This illustrates that the 6FNE-mediated response on the hippocampus is caused by selective α AR activation and not due to nonspecific AR effects. This also indicated that the 10 μ M concentration of timolol used to block β ARs was not interfering with this α AR-mediated response. Conversely, the EC_{50} of 6FNE, NE (1000 ± 310 nM, $n = 20$), and PHE (140 ± 130 μ M, $n = 12$) for reducing CA3 network activity were significantly less potent when evaluated against EPI (100 ± 12 nM, $n = 120$) or UK-14304 (76 ± 43 nM, $n = 10$), and were also significantly different when compared to each other (Fig. 3). Although UK-14304 was slightly more potent than EPI, the difference was not significantly different. The potency of EPI did not differ significantly over the age of animals (P12-P29) used in this study and was also not significantly different in adult rats versus juvenile animals (data not shown). This rank order of potency (UK-14304 \geq EPI > 6FNE > NE \gg PHE) is consistent with noradrenergic responses caused by α_2 AR activation.

Effect of Selective α AR Competitive Antagonists on the EPI Mediated Decrease in Discharge Frequencies. Functional determination of selective α AR antagonist equilibrium

dissociation constants (pK_b values) were used to characterize the type of α AR mediating decreased burst frequency in the hippocampal CA3 region (α_1 or α_2). Initially, CA3 field potential recordings generated by increasing amounts of EPI in the absence and presence of fixed concentrations of the highly selective α_2 AR antagonist atipamezole were used to shift the EPI concentration-response curve. Atipamezole possesses a greater than 1000-fold affinity for α_2 ARs when compared to α_1 ARs (Pertovaara et al., 2005). Hippocampal slices that had been pre-treated with 3, 10, 30 and 100 nM atipamezole produced 3-, 7-, 11- and 31-fold parallel rightward shifts of the fitted EPI concentration-response curve (Fig. 4A₁). Dose ratios calculated for individual runs were plotted against each atipamezole concentration to generate a straight line using linear regression analysis (Fig. 4A₂). The Schild regression slope included the value of unity (1.0 ± 0.1) and the x-intercept of the regression line represents the atipamezole equilibrium dissociation constant (pK_b) for the α AR subtype mediating the decreased burst frequency. The apparent calculated affinity value of 1.7 ± 0.5 nM ($n = 7$) was similar to previously published binding K_i values where atipamezole was used to identify α_2 ARs (Table 3).

Similar experiments were then used for determining the affinity of the selective α_1 AR antagonist prazosin to inhibit the EPI-mediated decrease in CA3 burst frequency. Hippocampal slices that had been pre-treated with 10, 20, 50 and 100 μ M prazosin produced 2-, 3-, 7- and 9-fold parallel rightward shifts of the fitted EPI concentration-response curve (Fig. 4B₁). Dose ratios were calculated and the Schild regression slope for prazosin (Fig. 4B₂) included the value of unity (1.0 ± 0.1) and the apparent calculated K_b was 4.9 ± 1.4 μ M ($n = 10$). This affinity value correlates most closely to previously reported equilibrium dissociation constants where prazosin was used to identify α_2 ARs (Table 3). Together, these K_b values for selective α AR antagonists confirm that α_2 AR activation is mediating this particular antiepileptic effect in CA3.

Effect of Subtype-Selective α_2 AR Competitive Antagonists on the EPI Mediated Decrease in Discharge Frequencies. To determine the specific subtype of α_2 AR involved in this response, apparent affinity values of subtype-selective α_2 AR competitive antagonists with different rank order of potencies for rat α_2 AR subtypes were determined using Schild regression analysis. Hippocampal slices pretreated with either ARC-239 (α_{2B} AR-selective), BRL-44408 (α_{2A} AR-selective), MK-912 (α_{2C} AR-selective), terazosin (α_{2B} AR-selective) or yohimbine (α_{2C} AR-selective), produced parallel rightward shifts of the fitted EPI concentration-response curve in all instances (data not shown). For each of these α_2 AR competitive antagonists, the slope of the regression line calculated using Schild regression analysis included the value of unity. The equilibrium dissociation constants (K_b values) calculated for these subtype-selective α_2 AR competitive antagonists were as follows: MK-912 (4.8 ± 1.6 nM, $n = 7$; slope = 1.0 ± 0.2), BRL-44408 (15 ± 9.4 nM, $n = 7$; slope = 1.1 ± 0.1), yohimbine (63 ± 15 nM, $n = 8$; slope = 1.1 ± 0.1), ARC-239 (540 ± 150 nM, $n = 8$; slope = 1.1 ± 0.1) and terazosin (5.0 ± 1.1 μ M, $n = 9$; slope = 1.1 ± 0.1). For each of these α_2 AR antagonists, the apparent calculated affinity value correlated most closely to published binding affinity value for the rat α_{2A} AR subtype than either the α_{2B} AR or α_{2C} AR subtypes (Table 3). Together, these results suggest the α_{2A} AR as the specific AR being activated by EPI to decrease hippocampal CA3 epileptiform burst frequency.

α_2 AR Antagonist Functional pK_b Estimates Correlate to α_{2A} AR Binding Affinity (pK_i) Values. A method frequently used to compare equilibrium dissociation constants of many receptor antagonists for a specific receptor is to correlate experimental affinity values with those that have been published previously (Bylund, 1988). Both the correlation coefficient and slope of the correlation line should be similar to unity if the calculated experimental values correspond to published constants for a specific receptor. Illustrated in Fig. 5 are the correlations between the functional affinity estimates (pK_b) determined for the selective α AR antagonists used in this

study and the previously published equilibrium dissociation constants (pK_i) of these AR antagonists for each rat α_2 AR subtype (see also Table 3). A poor correlation coefficient ($r = 0.32$) and line (slope = 0.21) was calculated when comparing our experimental pK_b values with previously published pK_i values for the rat α_{2B} AR (Fig. 5B, $n = 7$). Likewise, a poor correlation coefficient ($r = 0.70$) and a slope of 0.70 was calculated for the rat α_{2C} AR (Fig. 5C, $n = 6$). In contrast, a very high correlation coefficient (0.99) along with a slope of 1.0 was calculated for our experimental pK_b values when compared with published binding affinity values of these selective α AR antagonists for the rat α_{2A} AR subtype (Fig. 5A, $n = 6$). Either negative slope values or a poor correlation ($r < 0.50$) were calculated for the rat α_{1A} AR, α_{1B} AR and α_{1D} AR, respectively (data not shown). Together, these results indicate that, under conditions of impaired GABAergic inhibition, activation of α_{2A} ARs is primarily responsible for the antiepileptic actions of EPI in the rat hippocampal CA3 region.

Discussion

α_2 ARs expressed in the CNS have been implicated in the regulation of many critical brain processes, however, little is known about the mechanisms or involvement of specific α_2 AR subtypes. Building upon our previous findings (Jurgens et al., 2005), we confirmed that stimulation of an α_2 AR inhibits CA3 epileptiform activity induced by GABAergic inhibition. In this study, we also present molecular and functional evidence that this effect is primarily mediated through the α_{2A} AR subtype. These findings not only further our understanding for the role of NE in the CNS, but could have significant implications for the treatment of epilepsy.

Although *in situ* hybridization studies have shown the presence of transcripts for all three α_2 AR subtypes in the rat brain (Nicholas et al., 1993; Scheinin et al., 1994; Winzer-Serhan and Leslie, 1997; Winzer-Serhan et al., 1997a, b), these investigations were unable to resolve specific cell types expressing these receptors. Since previous pharmacological studies suggested α_2 ARs mediate the inhibition of CA3 network burst activity and this effect most likely results from activation of receptors located on hippocampal CA3 pyramidal cells (Jurgens et al., 2005), we utilized real time single cell RT-PCR methods to examine the subtype expression of α_2 AR mRNA transcripts. Genomic expression profiles suggested that α_{2A} AR and to a lesser extent α_{2C} AR activation could be involved in the inhibitory action of EPI on CA3 network burst activity. In the present study, α_{2A} AR transcripts were detected in 12 of 25 hippocampal CA3 pyramidal cells, three of which also co-expressed the α_{2C} AR transcript. The α_{2B} AR transcript was not detected in the cytoplasm harvested from the CA3 pyramidal cells. These results are in agreement with other studies indicating a greater expression of α_{2A} than α_{2C} AR mRNA in the rat hippocampal CA3 pyramidal layer, and no α_{2B} AR transcripts in the rat hippocampus (Scheinin et al., 1994; Winzer-Serhan and Leslie, 1997; Winzer-Serhan et al., 1997a, b). In contrast, Nicholas et al., 1993 found that there was more α_{2C} than α_{2A} AR mRNA in the rat hippocampal CA3 layer. It is possible that additional α_2 AR transcripts were present in our cytoplasmic

samples, but that their expression levels were below our detection limits since our RT-PCR primer pairs could only consistently amplify mRNA from > 1 pg of total RNA (data not shown).

Functional studies exploiting the selective properties of several AR agonists and antagonists were used to conclusively identify the α_2 AR inhibiting CA3 network burst activity. Application of the selective α_2 AR agonist UK-14304, the selective α AR agonist 6FNE or the non-selective AR agonists, NE or EPI, in the presence of β AR blockade caused a concentration-dependent decrease in the frequency of hippocampal CA3 burst discharges. In contrast, the selective α_1 AR agonist PHE did not elicit a significant antiepileptic effect until concentrations >100 μ M were tested. For this response, UK-14304 and EPI were found to have the highest potency of these tested AR agonists. The rank order of potency: UK-14304 \geq EPI > 6FNE > NE \gg PHE implies that α_2 AR populations, potentially those identified from single cell RT-PCR analysis, may be responsible for inhibiting hippocampal CA3 hyperexcitability.

Schild regression analysis allowed for calculation of equilibrium dissociation constants (K_b) of subtype-selective α_2 AR antagonists in order to identify which α_2 AR subtype(s) modulate the inhibition of CA3 hyperexcitability. Increasing concentrations of subtype-selective α_2 AR antagonists were used to produce parallel rightward shifts in the EPI concentration-response curve. These shifts occurred without significantly reducing maximal effects, demonstrating the competitive property of these subtype-selective α_2 AR antagonists. Using EC_{50} dose-ratios in the presence or absence of a selective α AR antagonist, Schild plots were constructed to determine the slope and x-intercept of the Schild regressions (Arunlakshana and Schild, 1959). Schild regression x-intercepts represent the K_b values of the α AR antagonists causing competitive inhibition of the EPI-mediated decrease in epileptiform burst discharge frequency.

The low apparent equilibrium dissociation constants (K_b values) calculated for the selective α_{2A} AR antagonist, BRL-44408, coupled with the high apparent K_b values determined for the selective α_{2B} AR antagonists (ARC-239, prazosin and terazosin) and selective α_{2C} AR

antagonists (MK-912 and yohimbine), support our belief that α_{2A} AR activation reduces CA3 hyperexcitability. Overall, the rank order of potency for these selective α AR antagonists (atipamezole > MK-912 > BRL-44408 > yohimbine > ARC-239 > prazosin \geq terazosin) was consistent with α_{2A} AR pharmacology described in other investigations (Table 3). Furthermore, our functionally determined pK_b values for α_2 AR inhibition of CA3 epileptiform activity correlated very closely ($r = 0.99$; slope = 1.0) with radioligand binding pK_i values determined for the α_{2A} AR, but not for the α_{2B} AR or α_{2C} AR (Fig. 5). Coupled with our single cell RT-PCR results which demonstrated that α_{2A} AR mRNA was most frequently detected in CA3 pyramidal cells, these findings indicate that an α_{2A} AR is responsible for EPI-mediated inhibition of CA3 epileptiform bursts under conditions of GABAergic blockade.

Inhibiting CA3 network bursts through stimulation of α_2 ARs may have profound effects on the generation and propagation of CA3 initiated seizures, such as in temporal lobe epilepsy. Noradrenergic activation has been shown to produce robust antiepileptic effects in a variety of seizure models (Giorgi et al., 2004). Conversely, reduced noradrenergic function increases seizure susceptibility. The α_2 AR is most often and consistently implicated in the antiepileptic effects of NE (Weinshenker and Szot, 2002). However, due to a lack of subtype-selective α_2 AR ligands, few studies have examined the specific α_2 AR subtype(s) involved. Recent studies using transgenic mice have suggested that α_{2A} ARs mediate NE's antiepileptic effects, as a point mutation of the α_{2A} AR abolishes the antiepileptogenic action of NE (Janumapalli et al., 1998) and the antiepileptic effects of α_2 AR agonists are absent in α_{2A} AR knockout mice (Szot et al., 2004). Interestingly, Szot et al. further concluded that the antiepileptic effects of NE were mediated by postsynaptic α_{2A} ARs. Our results provide evidence for a possible mechanism of postsynaptic α_{2A} AR mediated inhibition of epileptic activity through inhibition of a selective population of neurons in a specific region of the hippocampus (i.e., excitatory, glutamatergic

CA3 pyramidal cells). We suspect that a similar postsynaptic α_{2A} AR mediated inhibition of epileptiform activity may occur in other cortical structures which are often involved in seizures. Nonetheless, this particular hippocampal CA3 mechanism could potentially have profound effects on epilepsy as it would likely inhibit the spread of seizures through the hippocampus to other cortical structures.

Previous studies have shown that not only does NE fail to inhibit the normal glutamatergic transmission through the hippocampal CA3 circuitry, but it enhances synaptic plasticity in the hippocampal CA3 region (Hopkins and Johnston, 1988). Conversely, in this study, we have shown that NE eliminates hippocampal CA3 epileptiform burst discharges. To account for this, we hypothesize that α_{2A} AR activation reduces hippocampal CA3 epileptiform activity by decreasing the glutamate-mediated neurotransmission between pyramidal cells, but not the glutamatergic drive to or from the CA3 pyramidal cells (possibly by selectively inhibiting glutamate release from the recurrent collaterals). Additional experiments are currently being performed to confirm this hypothesis. If proven correct, this mechanism could explain in part how NE both enhances memory while maintaining its antiepileptogenic effects.

This hypothesis, that the α_{2A} AR-mediating the reduction in hippocampal CA3 epileptiform activity is located on the presynaptic glutamatergic terminals of the recurrent axon collaterals of the CA3 pyramidal neurons, could account for why we did not detect α_{2A} AR mRNA in CA1 pyramidal neurons (Table 2). If the role of the α_{2A} AR is to regulate (i.e., inhibit excessive) glutamate release from the recurrent collaterals, then we might expect no α_{2A} AR to be present in hippocampal CA1 pyramidal cells, as there is no recurrent network among the excitatory CA1 pyramidal neurons, as in CA3. Indeed, if α_{2A} ARs were inhibiting glutamate release either onto or from the CA1 pyramidal cells, then we would expect α_{2A} AR activation by NE to attenuate LTP and consequently, learning and memory, which is opposite from what has been observed. It is

nonetheless possible that α_2 AR transcripts were also present in the CA1 pyramidal cells, but that their expression levels were below the detection limits for the technique employed.

The present findings suggest a potential new pharmacotherapeutic strategy for treating epilepsy. Two major problems plaguing current antiepileptic medications are intolerable side effects such as attenuation of learning and memory and failure to adequately control seizures in a significant number of patients (Nadkarni et al., 2005). Evidence suggests, however, that unlike most current antiepileptic drugs, noradrenergic stimulation does not inhibit such cognitive functions as learning and memory (Devauges and Sara, 1991, Thomas and Palmiter, 1997) and may even facilitate certain types of memory processes (Murchison et al., 2004). In addition, indirect evidence suggests that a noradrenergic-based therapy could be effective against seizures that are refractory to current antiepileptic drugs. For example, vagus nerve stimulation, which is used to treat medically intractable epilepsies requires an intact NE system for its antiepileptic effects (Krahl et al., 1998), has also been shown to improve memory retention (Clark et al., 1999). Therefore, our results showing that an α_{2A} AR expressed on excitatory glutamatergic pyramidal cells inhibits hippocampal CA3 epileptiform activity offers the possibility of developing an noradrenergic-based therapy which prevents seizures without the adverse effect of interfering with learning and memory.

Acknowledgments

We thank Kendell Graywater, Kristan Green, Elisha Lawrence, Jamie Johnson, Jacob King, Vanessa Nelson, Trisha Sickler and Tiffany Stratton for help with the experiments and analyzing the data, and Karen Cisek for assistance in editing the manuscript.

V. REFERENCES

- Arunlakshana O and Schild HO (1959) Some quantitative uses of drug antagonists. *Br J Pharmacol* 14:48-58.
- Baf MH, Subhash MN, Lakshmana KM and Rao BS (1994) Alterations in monoamine levels in discrete regions of rat brain after chronic administration of carbamazepine. *Neurochem Res* 19:1139-1143.
- Bylund DB (1988) Subtypes of α_2 -adrenoceptors: pharmacological and molecular biological evidence converge. *Trends Pharmacol Sci* 9:356-61.
- Bylund DB, Eikenberg DC, Hieble JP, Langer SZ, Lefkowitz RJ, Minneman KP, Molinoff PB, Ruffolo RR Jr and Trendelenburg U (1994) International Union of Pharmacology nomenclature of adrenoceptors. *Pharmacol Rev* 46:121-136.
- Clark KB, Naritoku DK, Smitjh DC, Browning RA and Jensen RA (1999) Enhanced recognition memory following vagus nerve stimulation in human subjects. *Nat Neurosci* 2:94-98.
- Cleary L, Vandeputte C, Docherty JR (2003) Investigation of postjunctional α_1 - and α_2 -adrenoceptor subtypes in vas deferens from wild-type and α_{2AD} -adrenoceptor knockout mice. *Br J Pharmacol* 138:1069-1076.
- Devauges V and Sara SJ (1991) Memory retrieval enhancement by locus coeruleus stimulation: evidence for mediation by β -receptors. *Behav Brain Res* 43:93-97.
- Giorgi FS, Pizzanelli C, Biagioni F, Murri L and Fornai F (2004) The role of norepinephrine in epilepsy: from the bench to the bedside. *Neurosci Biobehav Rev* 28:507-524.
- Hancock AA, Buckner SA, Ireland LM, Knepper SM and Kerwin JF Jr (1995) Actions of terazosin and its enantiomers at subtypes of α_1 - and α_2 -adrenoceptors *in vitro*. *J Recept Signal Transduct Res* 15:863-885.

- Haapalinna A, Viitamaa T, MacDonald E, Savola J-M, Tuomisto L, Virtanen R, and Heinonen E (1997) Evaluation of the effects of a specific α_2 -adrenoceptor antagonist, atipamezole, on α_1 - and α_2 -adrenoceptor subtype binding, brain neurochemistry and behaviour in comparison with yohimbine. *Naunyn-Schmiedeberg's Arch Pharmacol* 356:570-582.
- Harrison JK, D'Angelo DD, Zeng D and Lynch KR (1991) Pharmacological characterization of rat α_2 -adrenoceptor receptors. *Mol Pharmacol* 40:407-412.
- Hillman KL, Doze VA and Porter JE (2005a) Adrenergic receptor characterization of CA1 hippocampal neurons using real time single cell RT-PCR. *Brain Res Mol Brain Res* 139:267-276.
- Hillman KL, Doze VA and Porter JE (2005b) Functional characterization of the β -adrenergic receptor subtypes expressed by CA1 pyramidal cells in the rat hippocampus. *J Pharmacol Exp Ther* 314:561-567.
- Hopkins WF and Johnston D (1988) Noradrenergic enhancement of long-term potentiation at mossy fiber synapses in the hippocampus. *J Neurophysiol* 59:667-687.
- Janumpalli S, Butler LS, MacMillan LB, Limbird LE and McNamara JO (1998) A point mutation (D79N) of the α_{2A} -adrenergic receptor abolishes the antiepileptogenic action of endogenous norepinephrine. *J Neurosci* 18:2004-2008.
- Jurgens CWD, Boese SJ, King JD, Pyle SJ, Porter JE and Doze VA (2005) Adrenergic receptor modulation of hippocampal CA3 network activity. *Epilepsy Res* 66:117-128.
- Kenakin T (1997) Competitive Antagonism, in *Pharmacologic Analysis of Drug-Receptor Interaction* (Kenakin T ed) 3rd ed, pp 331-373, Lippincott-Raven, Philadelphia.
- Kesner RP, Lee I and Gilbert P (2004) A behavioral assessment of hippocampal function based on subregional analysis. *Rev Neurosci* 15:333-351.
- Krahl SE, Clark KB, Smith DC and Browning RA (1998) Locus coeruleus lesions suppress the seizure-attenuating effects of vagus nerve stimulation. *Epilepsia* 39:709-714.

- Lu S-F, Herbert B, Haufe G, Laue KL, Padgett WL, Oshumleti O, Daly JW and Kirk KL (2000) Syntheses of (R) - and (S)-2- and 6-fluoronorepinephrine and (R) - and (S)-2- and 6-fluoroepinephrine: Effect of stereochemistry on fluorine-induced adrenergic selectivity's. *J Med Chem* 43:1611-1619.
- Murchison CF, Zhang XY, Zhang WP, Ouyang M, Lee A and Thomas SA (2004) A distinct role for norepinephrine in memory retrieval. *Cell* 117:131-143.
- Nadkarni S, LaJoie J and Devinsky O (2005) Current treatments of epilepsy. *Neurology* 64:S2-11.
- Nicholas AP, Pieribone V and Hokfelt T (1993) Distributions of mRNAs for α -2 adrenergic receptor subtypes in rat brain: an *in situ* hybridization study. *J Comp Neurol* 328:575-594.
- O'Rourke MF, Iverson LJ, Lomasney JW and Bylund DB (1994) Species orthologs of the *alpha*-2A adrenergic receptor: The pharmacological properties of the bovine and rat receptors differ from the human and porcine receptors. *J Pharmacol Exp Ther* 271:735-740.
- Patane MA, Scott AL, Broten TP, Chang RSL, Ransom RW, DiSalvo J, Forray C, and Bock MG (1998) 4-Amino-2-[4-[1-(benzyloxycarbonyl)-2(S)-[[[(1,1-dimethylethyl)amino]carbonyl]-piperazinyl]-6,7-dimethoxyquinazoline (L-765,314): A potent and selective α_{1b} adrenergic receptor antagonist. *J Med Chem* 41:1205-1208.
- Pertovaara A, Haapalinna A, Sirviö J and Virtanen R (2005) Pharmacological properties, central nervous effects, and potential therapeutic applications of atipamezole, a selective α_2 -adrenoceptor antagonist. *CNS Drug Rev* 11:273-288.
- Pupo AS and Minneman KP (2001) Adrenergic pharmacology: focus on the central nervous system. *CNS Spectr* 6:656-662.
- Schwartzkroin PA (1986) Hippocampal slices in experimental and human epilepsy, in *Advances in Neurology, vol 44, Basic Mechanisms of the Epilepsies* (Delgado-Escueta AV ed) pp 991-1010, Raven Press, New York.

- Scheinin M, Lomasney JW, Hayden-Hixson DM, Schambra UB, Caron MG, Lefkowitz RJ and Fremeau RT Jr (1994) Distribution of α_2 -adrenergic receptor subtype gene expression in rat brain. *Mol Brain Res* 21:133-149.
- Szot P, Lester M, Laughlin ML, Palmiter RD, Liles LC and Weinshenker D (2004) The anticonvulsant and proconvulsant effects of α_2 -adrenoreceptor agonists are mediated by distinct populations of α_{2A} -adrenoreceptors. *Neuroscience* 126:795-803.
- Szot P, Weinshenker D, Rho JM, Storey TW and Schwartzkroin PA (2001) Norepinephrine is required for the anticonvulsant effect of the ketogenic diet. *Brain Res Dev Brain Res* 129:211-214.
- Thomas SA and Palmiter RD (1997) Disruption of the dopamine beta-hydroxylase gene in mice suggests roles for norepinephrine in motor function, learning, and memory. *Behav Neurosci* 111:579-589.
- Traub RD, Wong RK, Miles R and Michelson H (1991) A model of a CA3 hippocampal pyramidal neuron incorporating voltage-clamp data on intrinsic conductances. *J Neurophysiol* 66:635-650.
- Uhlén S and Wikberg JES (1991) Delineation of rat kidney α_{2A} - and α_{2B} -adrenoceptors with [3 H]-RX821002 radioligand binding: computer modeling reveals that guanfacine is an α_{2A} -selective compound. *Eur J Pharmacol* 202:235-243.
- Uhlén S, Xia Y, Chhajlani V, Felder CC and Wikberg JES (1992) [3 H]-MK 912 binding delineates two α_2 -adrenoceptor subtypes in rat CNS one of which is identical with the cloned pA2d α_2 -adrenoceptor. *Br J Pharmacol* 106:986-995.
- Weinshenker D and Szot P (2002) The role of catecholamines in seizure susceptibility: new results using genetically engineered mice. *Pharmacol Ther* 94:213-233.

- Weiss GK, Lewis J, Jimenez-Rivera C, Vigil A and Corcoran ME (1990) Antikindling effects of locus coeruleus stimulation: mediation by ascending noradrenergic projections. *Exp Neurol* 108:136-140.
- Winzer-Serhan UH and Leslie FM (1997) α_{2A} adrenoceptor mRNA expression during rat brain development. *Dev Brain Res* 100:90-100.
- Winzer-Serhan UH, Raymon HK, Broide RS, Chen Y and Leslie FM (1997a) Expression of α_2 adrenoceptors during rat brain development – I. α_{2A} messenger RNA expression. *Neuroscience* 76:214-260.
- Winzer-Serhan UH, Raymon HK, Broide RS, Chen Y and Leslie FM (1997b) Expression of α_2 adrenoceptors during rat brain development – II. α_{2C} messenger RNA expression and [3 H]rauwolscine binding. *Neuroscience* 76:214-260.

VI. FOOTNOTES

Source of financial support: This investigation was supported in part by North Dakota Experimental Program to Stimulate Competitive Research (ND EPSCoR) through National Science Foundation (NSF) Grants EPS-0132289 and EPS-0447679 (to V.A.D.), NSF Faculty Early Career Development (CAREER) Award Grant 0347259 (to V.A.D.), National Institutes of Health Grant 2P20RR016471 from the Biomedical Research Infrastructure Networks (BRIN) program and National Institutes of Health Grant 5P20RR017699 from the Centers of Biomedical Research Excellence (COBRE) program (to V.A.D. and J.E.P.). Additional student support was provided by an Epilepsy Foundation Predoctoral Research Training Fellowship (to C.W.J.), an American Epilepsy Society Predoctoral Research Training Fellowship (to K.L.H.), a Doctoral Dissertation Assistantship from ND EPSCoR (to K.L.H.), an Advanced Undergraduate Research Award (AURA) from ND EPSCoR (to S.J.B), an Explorations in Biomedicine Undergraduate Summer Research Fellowship for Native Americans from the American Physiological Society (to K.L.D.), and an Undergraduate Summer Research Training Fellowship from the University of North Dakota Office of the Associate Vice President for Medical Research (to B.L.G. and J.A.L.).

Citation of meeting abstracts: A preliminary report of these findings was presented at the 2005 annual meeting of the Society for Neuroscience, November 12-16, Washington D.C. and the 2006 annual meeting of the American Society for Pharmacology and Experimental Therapeutics, Neuropharmacology Session, April 1-5, San Francisco.

Person to receive reprint requests: Dr. Van A. Doze, Department of Pharmacology, Physiology and Therapeutics, School of Medicine and Health Sciences, University of North Dakota, 501 North Columbia Road, Grand Forks, ND 58203, E-mail address: vdoze@medicine.nodak.edu.

¹Current affiliation: Department of Pharmaceutical Sciences, School of Pharmacy, North Dakota State University, Fargo, North Dakota.

²These authors contributed equally to this work.

VII. LEGENDS FOR FIGURES

Fig. 1. Hippocampal slice preparation and single cell cytoplasmic extraction. **A**, schematic diagrams of the rat brain and hippocampal formation. Illustrated are the location of hippocampus in the rat brain (bottom) and the basic neuronal organization of the rat hippocampal formation (top). **Bottom diagram**, illustrates the orientation used in preparing hippocampus slices from the rat brain. Hippocampi were carefully dissected from the brain, positioned on moistened filter paper, and cut into 500 μm thick slices. For these recordings, the slices were cut at a slight angle (about 15 degrees) off the transverse. **Top diagram**, shows details of the rat hippocampal slice formation and the placement of the extracellular recording electrode. The major regions of the rat hippocampus are the dentate gyrus (DG), area CA3 and area CA1. To record epileptiform burst discharges, the extracellular recording electrode was placed directly in the pyramidal neuron layer (stratum pyramidale) in the region of the area CA3. **B**, pictured is an IR-DIC image of a visually identified hippocampal CA3 pyramidal cell prior to cytoplasmic extraction. Arrow indicates cell soma. Note microelectrode touching the membrane of the candidate pyramidal cell.

Fig. 2. Effects of 6FNE on hippocampal CA3 epileptiform burst discharges. **A**, continuous 150 s-long chart recordings of burst discharges recorded in the hippocampal CA3 region of rat brain slices. Burst discharges were elicited by including 100 μM of the GABA_A receptor blocker picrotoxin in the perfusing ACSF containing 500 nM desipramine. Under these conditions, bath application of 6FNE reduced burst frequency in a concentration-dependent manner from 12 bursts (0.080 Hz) in control ringer to 9 (0.060 Hz) in 30 nM, 7 (0.047 Hz) in 100 nM, 4 (0.027 Hz) in 300 nM, 2 (0.013 Hz) in 1 μM , and 1 (0.007 Hz) in 3 μM 6FNE. The effect of 6FNE was completely reversible in that the frequency of events returned to baseline level after several

washes with control ACSF (data not shown). **B**, frequency histogram of the number of epileptiform burst discharges versus time of 6FNE application. Each bin represents the frequency averaged over a 150-s epoch. Increasing concentrations of 6FNE were applied to the bath for the 8 min periods indicated. **Inset**, concentration-response curve derived from the frequency histogram in panel B. Data points were plotted as percent of maximal inhibition (decrease in epileptiform burst frequency) and the curve constructed using a nonlinear least-squares curve-fitting method. For this experiment, the concentration-response curve was fit best by a nonvariable sigmoidal model with a calculated EC_{50} value for 6FNE of 110 nM. **C**, mean concentration-response curve for all of the 6FNE data (310 ± 86 nM; $n = 20$).

Fig. 3. Rank order of potency for EPI, 6FNE, NE and PHE inhibiting hippocampal CA3 epileptiform burst activity. Extracellular field potentials were used to generate concentration-response curves using increasing amounts of UK-14304 (●), EPI (○), 6-FNE (■), NE (□), and PHE (▲) in the presence of 10 μ M timolol and 0.5 μ M desipramine. There was no significant difference between the calculated EC_{50} value for UK-14304 (76 ± 43 nM, $n = 10$) and EPI (100 ± 12 nM, $n = 120$). There was a significant difference in the potencies calculated for UK-14304 or EPI, compared to 6FNE (300 ± 140 nM, $n = 12$), NE (1.0 ± 0.31 μ M, $n = 20$) or PHE (140 ± 130 μ M, $n = 12$). There also was a significant difference between the EC_{50} for 6FNE versus NE, 6FNE versus PHE, and NE versus PHE. Concentration-response curves for each agonist were plotted as percent of maximal response (decrease in epileptiform burst frequency). Each individual experiment best fit to a non-variable sigmoidal curve.

Fig. 4. Schild regression analysis using α AR antagonists. **A₁**, consecutive EPI concentration-response curves demonstrate a concentration-dependent effect of the selective α_2 AR antagonist atipamezole. Pre-treatment with 3 nM (○), 10 nM (■), 30 nM (□) and 100 nM

(▲) of this AR antagonist produced consecutive parallel rightward shifts of the EPI curve that were significantly different from control (●) ($EC_{50} = 330 \pm 72, 780 \pm 270, 1200 \pm 430, \text{ and } 3500 \pm 4400$ respectively, versus 110 ± 31 nM for control). **A₂**, using dose ratios calculated from individual experiments illustrated in **A₁**, a Schild plot was created generating a regression slope equaling 1.0 ± 0.1 and an x-intercept correlating to a K_b value of 1.7 ± 0.5 nM ($n = 7$). **B₁**, pre-treatment with 10 μM (○), 20 μM (■), 50 μM (□) and 100 μM (▲) of the selective $\alpha_1\text{AR}$ antagonist prazosin, produced consecutive parallel rightward shifts of the EPI curve that were significantly different from control (●) ($EC_{50} = 150 \pm 46, 230 \pm 48, 520 \pm 89, \text{ and } 710 \pm 140$ respectively, versus 78 ± 24 nM for control). **B₂**, using dose ratios calculated from individual experiments illustrated in Panel **B₁**, a Schild plot was created generating a regression slope equaling 1.1 ± 0.1 and an x-intercept correlating to a K_b value of 4.9 ± 1.4 μM ($n = 10$).

Fig. 5. Correlation between functional pK_b estimates and binding affinity (pK_i) values for various selective αAR antagonists. Using the pK_i values for rat $\alpha_2\text{ARs}$ (see Table 3), correlation analyses were performed for **A**, the $\alpha_{2A}\text{AR}$, **B**, the $\alpha_{2B}\text{AR}$, and **C**, the $\alpha_{2C}\text{AR}$. The correlation coefficient and slope was 0.99 and 1.0 for the $\alpha_{2A}\text{AR}$, 0.32 and 0.21 for the $\alpha_{2B}\text{AR}$, and 0.70 and 0.70 for the $\alpha_{2C}\text{AR}$.

VIII. TABLES

TABLE 1. Gene-specific primers used in RT-PCR

Gene	Genebank accession number	Forward Reverse Oligonucleotide Sequence [5' → 3']	Product size (bp)	Melt temp (°C)
β -Actin ^a	V01217	TTTGAGACCTTCAACACCCCAGCCAT ATGTCACGCACGATTTCCCTCTCA	266	88
CaMKII	NM_012920	TGGAGGCTGTGCTACACTGTCACCAG CTGCTGGTACAGGCGGTGCTGGTC	314	89
GAD65	M72422	TGGGTGTCCCCTTGCAATGTTCCG AGTAGTCCCCTTTGCTCTCCACATGA	203	89
GFAP	L27219	TCCTTCTGTTTTTATGCCACGGC ATGTTTTCTTTCTGTCT	308	87
α_{2A} AR	NM_012739	CGTGGTGTGTTGGTTCCCGTTCTTTT CGGCAGAGGATCTTCTTGAAGGC	180	89
α_{2B} AR	NM_138505	AGAGGAGGGAGATGAAGAGGATGAGG AAGACGGTGTAGATGACAGGGTTCAAA	399	89
α_{2C} AR	NM_138506	TTCGTA CTGTGCTGGTTCCCCTTCTTCTTC TCCTACGGAAGAGGATGTGCTTGAAAG	196	89

^aHouse keeping gene. The genomic primer recognized the polymorphic repeat STS ET3 (Forward, GCCTGCATTCATCTTCATCTGC; Reverse, AAAGGTGGA ACTCGCCCGTTT).

TABLE 2. Single Cell RT-PCR results for rat hippocampal pyramidal neurons

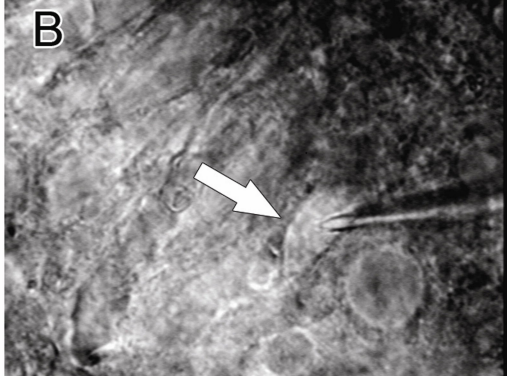
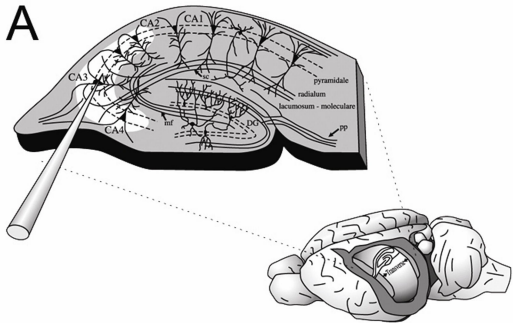
	α_{2A} AR	α_{2B} AR	α_{2C} AR
CA3 cells	12 / 25	0 / 25	3 / 25

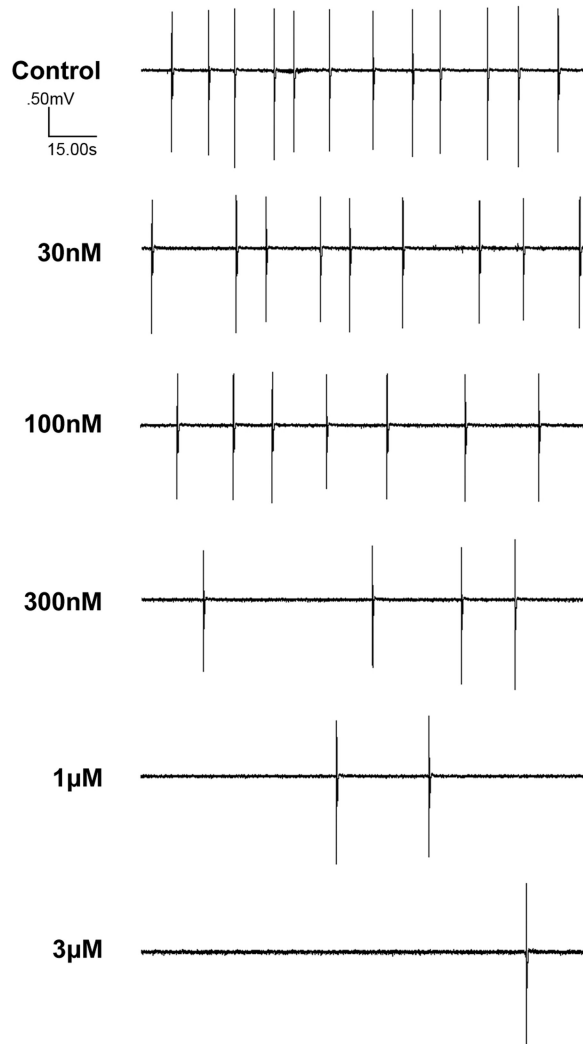
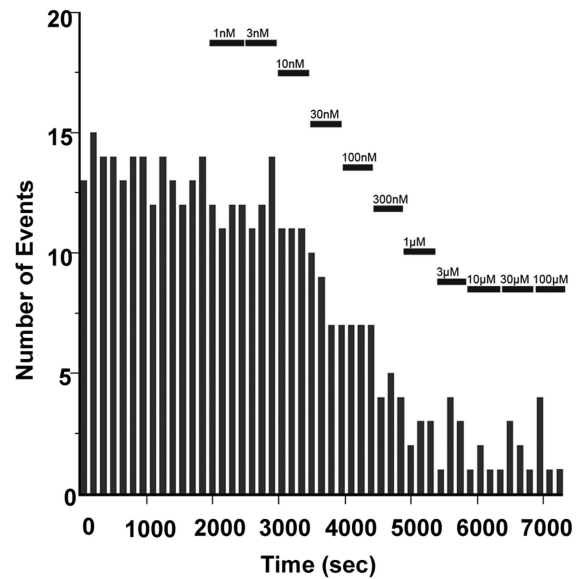
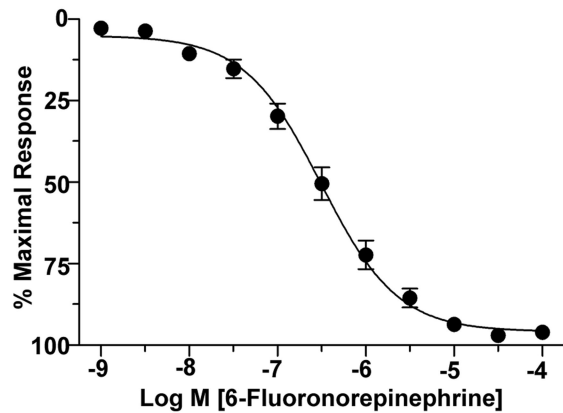
Data are from cell samples that were positive for the housekeeping gene β -actin and negative for the genomic marker STS ET3, indicating successful amplification of cytoplasmic mRNA.

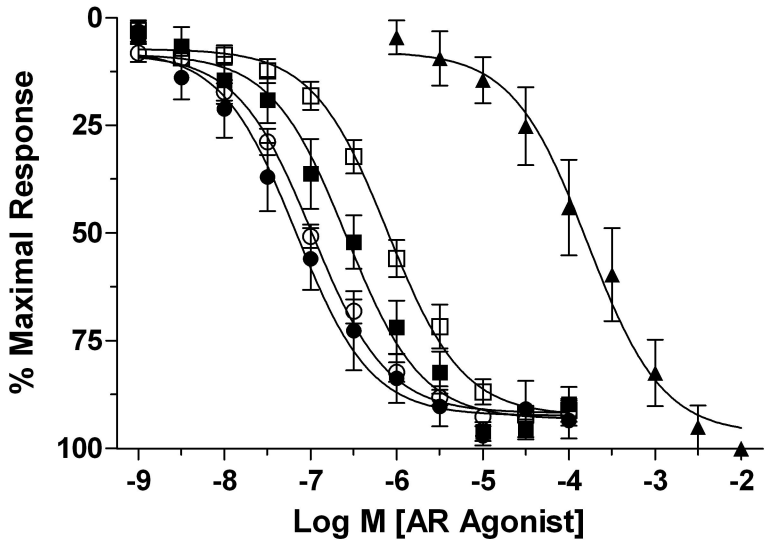
TABLE 3. Comparisons of functional K_b values to previously published equilibrium dissociation constants (K_i) of selective α AR antagonists for rat α AR subtypes

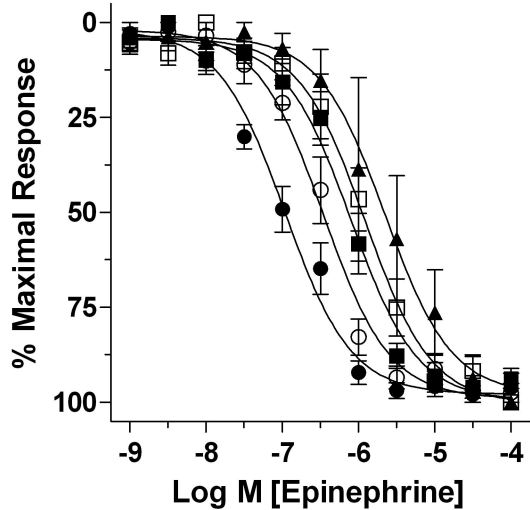
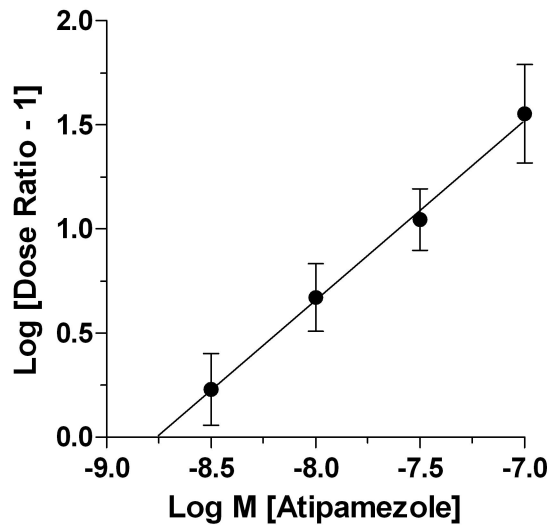
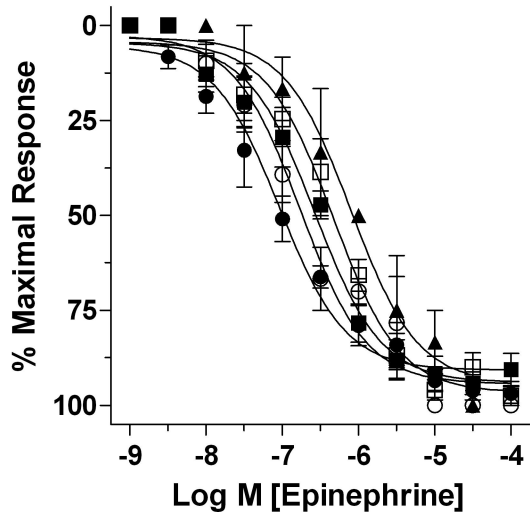
Antagonist	K_b (nM)	Reported K_i Values (nM)					
		α_{2A}	α_{2B}	α_{2C}	α_{1A}	α_{1B}	α_{1D}
Atipamezole	1.7 ± 0.5	1.1 ^a	1.0 ^a	0.89 ^a	1300 ^{f*}	6500 ^{f*}	n/a
MK-912	4.8 ± 1.6	2.5 ^{b*}	1.3 ^{b*}	0.046 ^c	n/a	n/a	n/a
BRL-44408	15 ± 9.4	14 ^{b*}	480 ^{b*}	74 ^c	270 ^{g*}	n/a	n/a
Yohimbine	63 ± 15	43 ^a	6.9 ^a	2.6 ^a	n/a	660 ^{h*}	n/a
ARC-239	540 ± 150	750 ^d	14 ^{b*}	47 ^c	n/a	n/a	0.39 ^e
Prazosin	4900 ± 1400	2500 ^a	36 ^a	80 ^a	0.3 ⁱ	0.2 ⁱ	0.3 ⁱ
Terazosin	5000 ± 1100	n/a	7.8 ^{e*}	n/a	3.9 ⁱ	1.9 ⁱ	3.4 ⁱ

K_b values are expressed as the mean ± S.E. Schild regression slopes are expressed as the mean slope ± S.E. and were determined in seven to ten separate experiments. K_i values are from binding studies using recombinant rat α AR clones expressed in cell lines. * K_i from rat tissues were used if no rat α AR clone data was available; n/a, not available. ^aHarrison et al. (1991); ^bÚhlen and Wikberg (1991); ^cÚhlen et al. (1992); ^dO'Rourke et al. (1994); ^eHancock et al. (1995); ^fPertovaara et al. (2005); ^gCleary et al. (2003); ^hHaapalinna et al. (1997); ⁱPatane et al. (1998).



A**B****C**



A₁**A₂****B₁****B₂**